Philippe Büchler[1]
ARTORG Center for Biomedical Engineering Research, University of Bern, Bern 3010, Switzerland
e-mail: philippe.buechler@artorg.unibe.ch

Jonas Räber
Institute of Mechanical Engineering and Energy Technology, Lucerne School of Engineering and Architecture, Luzern 6002, Switzerland
e-mail: raeber.jonas@gmail.com

Benjamin Voumard
ARTORG Center for Biomedical Engineering Research, University of Bern, Bern 3010, Switzerland
e-mail: benjamin.voumard@artorg.unibe.ch

Steve Berger
ARTORG Center for Biomedical Engineering Research, University of Bern, Bern 3010, Switzerland
e-mail: steve.berger.steve.berger@gmail.com

Brett Bell
ARTORG Center for Biomedical Engineering Research, University of Bern, Bern 3010, Switzerland
e-mail: biobrettbell@gmail.com

Nino Sutter
ARTORG Center for Biomedical Engineering Research, University of Bern, Bern 3010, Switzerland
e-mail: nino.sutter@gmx.net

Stefan Funariu
ARTORG Center for Biomedical Engineering Research, University of Bern, Bern 3010, Switzerland
e-mail: funariu@gmx.net

Carol Hasler
Orthopaedic Department, Children's Hospital, University of Basel, Basel 4056, Switzerland
e-mail: carolclaudius.hasler@ukbb.ch

Daniel Studer
Orthopaedic Department, Children's Hospital, University of Basel, Basel 4056, Switzerland
e-mail: daniel.studer@ukbb.ch

The Spinebot—A Robotic Device to Intraoperatively Quantify Spinal Stiffness

Degenerative spine problems and spinal deformities have high socio-economic impacts. Current surgical treatment is based on bony fusion that can reduce mobility and function. Precise descriptions of the biomechanics of normal, deformed, and degenerated spinal segments under in vivo conditions are needed to develop new approaches that preserve spine function. This study developed a system that intraoperatively measures the three-dimensional segmental stiffness of patient's spine. SpineBot, a parallel kinematic robot, was developed to transmit loads to adjacent vertebrae. A force/torque load cell mounted on the SpineBot measured the moment applied to the spinal segment and calculated segmental stiffnesses. The accuracy of SpineBot was characterized ex vivo by comparing its stiffness measurement of five ovine specimens to measurements obtained with a reference spinal testing system. The SpineBot can apply torques up to 10 N·m along all anatomical axes with a total range of motion of about 11.5 deg ± 0.5 deg in lateral bending, 4.5 deg ± 0.3 deg in flexion/extension, and 2.6 deg ± 0.5 deg in axial rotation. SpineBot's measurements are noisier than the reference system, but the correlation between SpineBot and reference measurements was high ($R^2 > 0.8$). In conclusion, SpineBot's accuracy is comparable to that of current reference systems but can take intraoperative measurements. SpineBot can improve our understanding of spinal biomechanics in patients who have the pathology of interest, and take these measurements in the natural physiological environment, giving us information essential to developing new "nonfusion" products.
[DOI: 10.1115/1.4049915]

[1]Corresponding author.
Manuscript received September 18, 2020; final manuscript received December 17, 2020; published online February 9, 2021. Assoc. Editor: Nandini Duraiswamy.

Introduction

Back pain and degenerative spine problems are the main reasons people stop working and take early pensions, and the most common reason for back surgery [1–3]. Their already high social and economic costs will increase as the population ages. Even in young people with scoliosis, operative treatment generally fuses the bone in deformed sections of the spinal column. This method stabilizes the spine with metallic implants so motion segments can ossify. New strategies for preserving or restoring spine function include artificial discs, interspinous process spacers, posterior transpedicular dynamic stabilization, and target-oriented conservative approaches. These new technologies could be used for better advantage if we knew more about the kinematic and dynamic properties of the spine, and especially the complex force–motion relationship in normal, degenerative, and scoliotic spinal segments under in vivo conditions.

Ex vivo testing on spinal loading simulators (SLSs) has been the near exclusive standard for biomechanical spine assessment and analysis of spine stiffness [4–10]. Pure bending moments are applied on isolated spinal segments to simulate relevant spinal loading [11]. This method has improved general understanding of normal spine function and the consequences of induced injuries, but it is an ex vivo experiment and appropriate human cadaver spines are scarce. Most are extracted from the cadavers of the elderly and rarely exhibit the pathology of interest. Thus, this method provides information of limited value for doctors who must make clinical decisions, and for patients.

Several studies addressed these issues by describing spinal biomechanics based on intraoperative tests [12–19]. They differ by the tools they used to generate force, by the loci to which force was applied, and by how, and in which planes they recorded motion. These studies restricted force application and motion recording to the sagittal plane. Exact intrasegmental motions of the vertebrae were not captured during the distraction and no method considered complex three-dimensional vertebral motion; thus, none of these tools measured spinal stiffness along all three anatomical axes.

An alternative approach was proposed by Rohlmann et al., measuring the load on the anterior spinal column in vivo with a modified instrumented vertebral body replacement [20–23]. This technique accurately measures forces and torque induced in the disc during daily activities, but it is limited to patients who need vertebral body replacement; uninstrumented segments cannot be assessed and the procedure may cause complications. The approach also cannot quantify the stiffness of the motion segment because it only measures force and not the resulting force-induces vertebral motion.

One instrumented forceps was combined with an optical tracking system to measure the motion of the vertebras when the load was applied [24]. It was used intraoperatively to quantify the segmental stiffness of scoliotic patients [25], but it had several limitations: the load was applied on the transverse processes, which mainly induces lateral bending and a small amount of flexion; it produced no axial rotation so it provided no information on spinal stiffness in rotation; and, the system was manually operated, which limits its reproducibility and the accuracy of its stiffness measurements.

To learn more about the biomechanics of the pathological spine, we must take intraoperative in vivo measurements that will provide direct, reproducible, and accurate information about the multi-axial load–displacement behavior of the functional spinal unit. This mechanical characterization can be used to improve intraoperative decision-making and develop new therapeutic strategies and implants. We thus developed a robotic system that accurately quantifies spinal stiffness intraoperatively.

Materials and Methods

The SpineBot. The SpineBot is a compact ($9 \times 9 \times 25\,\text{cm}^3$), lightweight (1.8 kg) robotic device (Fig. 1) based on a Stewart platform—a six degrees-of-freedom parallel kinematic structure based on six extensible linear actuators. The custom-made actuators use standard brushless DC motors (Faulhaber Minimotor SA, series 1226 012B, Croglio, Switzerland) and gearbox (Faulhaber Minimotor SA, Spur gearheads zero backlash, series 12/5, 69.2:1, Croglio, Switzerland) that are connected to a ball screw with a belt (MPS Micro-Precision Systems SA, ED410X/V4121X, Switzerland). Each actuator is connected to a base plate and a platform that has spherical joints at each end (B7104 MSS 2Z, SBN Wälzlager GmbH, Schönenberg-Kübelberg, Germany).

The SpineBot is attached to the patient's spine with bilateral pedicle screws inserted in each vertebra as part of the standard spinal intervention. We developed a flexible system based on a polyaxial attachment to make it possible to fix the platform to the spine for any possible positioning of the pedicle screws. A quick release mechanism is mounted on the attachment structure to make it easy to clamp the robot on the patient before taking measurements. Most important, the SpineBot can be immediately detached in case of emergency. The lower part of the two-part quick release mechanism is mounted to the attachment platform; the upper part is attached to the SpineBot. Active air pressure of 4.5 bars clamps the SpineBot on the attachment structure. Compressed air accumulates in a chamber inside the quick release

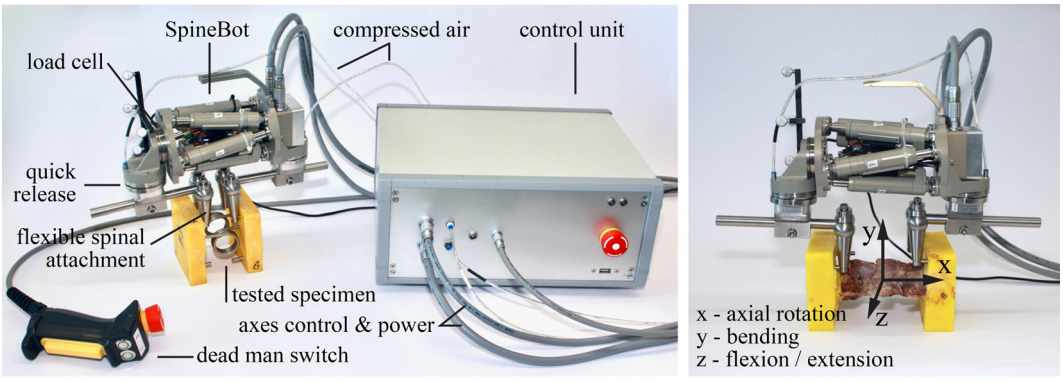

(*a*) (*b*)

Fig. 1 (*a*) The complete SpineBot system showing the robot attached to a validation spring, the control unit, and the dead-man switch. (*b*) The robot attached to an ovine spinal segment. Vertebras adjacent to the tested segments were embedded in PMMA blocks to enable the spinal loading simulator to measure stiffness. The coordinate system indicates the main anatomical directions used to evaluate spinal stiffness. Flexion/extension rotates around axis *z*, lateral bending around axis *y*, and axial rotation around *x*. Note that axis *y* (lateral bending) passes through the SpineBot, the other two axes do not.

system; the air pushes a token, which changes the orientation of three locking elements that fasten the SpineBot to the attachment structure. The system is fail-safe; if the air pressure drops—deliberately or if the system fails—the SpineBot automatically detaches from the patient. The pressure valve also automatically opens when power is interrupted.

To avoid any measurement bias caused by the weight of the SpineBot on the patient's spine, stiffness measurements are performed with the SpineBot attached to a weight canceling platform. A cable is used to apply a vertical traction force aligned with the center of mass of the robot. The cable is connected to a canceling mass through a pulley place above the robot. This platform also ensures that the SpineBot completely disconnects from the patient in the event of an emergency interruption, and that it does not fall on the patient.

The robot can only move if a human actively and constantly presses on the remote dead-man switch (Fig. 1). If the dead-man switch is released, the robot stops moving and, if the dead man switch is pressed strongly, air pressure is interrupted and the SpineBot detaches from the spine.

A force/torque load cell (Mini45-AE Transducer, ATI industrial automation, NC) is mounted on the base platform to measure the load the device applies on the spinal motion segments. The load cell was industrially calibrated (SI-290-10); its range of force measurement is 290 N along the x and y directions and 580 N in the z direction, at a resolution of 0.125 N. The range of moment measurement is $\pm$ 10 N·m at resolution of 1/376 N·m along x and y, and 10 N·m at a resolution of 1/752 N·m for the torque along z (Fig. 2). The motors and load cell are wired to the robot control unit that contains the motor controller (Technosoft iPOS3602 VX, Technosoft SA, Neuchâtel, Switzerland), the power supply, and an industrial PC that runs the controller software.

A separate microcontroller (the watchdog) periodically receive handshake from each subsystem. If a handshake fails—indicating that a component is in an error state—the air pressure of the quick release mechanism is cut.

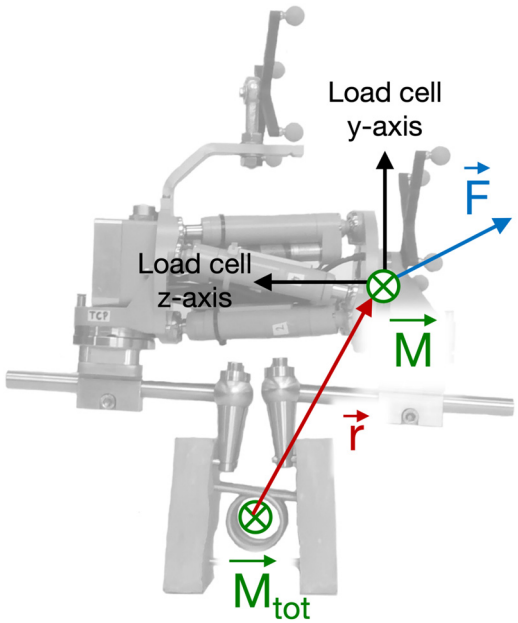

Fig. 2 Free body diagram for calculating spinal stiffness from measurements taken by the force/torque sensor. The load cell mounted on the robot measures both the force and moment vectors the SpineBot applies to the vertebras. The calculation of the total moment at the center of the motion segment being tested must account for the moment arm of the forces (1).

SpineBot Control. The length and orientation of all the actuators can be calculated from the position and orientation of the platform—inverse position kinematics—based on geometric relationships. Since there is no closed form solution to calculate the position and orientation of the platform from the length of the actuators—forward kinematics—we used an iterative scheme to calculate the real-time forward kinematics solution [26]. The software controller (written in C++) determines the position of the axes and constantly communicates the new position of each axis to the hardware controllers via a controller area network interface.

Before taking measurements, the robot is detached from the patient to conduct a "homing" procedure. All axes are moved to their shortest configuration to give the controller their reference positions. A limit switch (IFFM 04P1501/O1 L, Baumer, Electric AG, Frauenfeld, Switzerland) determines the zero-length reference position of the axes; it is fixed to the side of the housing and detects when the ball screw reaches its lower limit. When the limit switch is activated, the linear actuator reaches its minimal length. From this position, the SpineBot is positioned with the axis elongated to the middle of its possible extension. A haptic mode manually positions the robot on the patient. Zero impedance control was used to easily position and align both sides of the robot on the quick release mechanism. Once correctly positioned, activating the air pressure fixes the SpineBot firmly on the spine.

Stiffness Calculation. The position of the spine relative to the SpineBot is determined with a registration procedure. A series of landmarks are identified on the SpineBot and on three-dimensional models of the spine reconstructed from CT imaging. The position of these landmarks is identified before measurement using a pointer and an optical tracking system (Polaris, Northern Digital, Inc., Waterloo, ON, Canada); this enables to define the main anatomical direction in the coordinate system of the SpineBot. The information is fed back to the SpineBot to define the loading scheme along these anatomical axes.

The SpineBot is programed to apply a motion along the main anatomical axes; flexion/extension; lateral bending; and, axial rotation (Fig. 1(*b*)). Mechanical stiffness in each direction is calculated as the ratio between the measured moment and rotation angle. To precisely quantify the moment applied on the spinal segment, a pure moment must be applied on the specimen tested, so the SpineBot must only apply moments on the spine, and cancel all parasitic forces (Fig. 2). The force is canceled by a proportional–integral–derivative (PID) controller that adapts the motion of each axis to ensure that the forces the force/torque load cell measures remain at zero while the measurements are taken.

Spinal stiffness must be calculated at the center of the spinal motion segment located at the approximate center of the intervertebral disc. Both the rotation, and the moment the SpineBot applies must be calculated at this position (Fig. 2) with the following equation:

$$\mathbf{M}_{\mathrm{TOT}} = \mathbf{M} + \mathbf{r} \times \mathbf{F} \tag{1}$$

where $\mathbf{r}$ is the vector between the center of the vertebra and the load cell, $\mathbf{F}$ and $\mathbf{M}$ and are the force vector and moment measured by the load cell. The force $\mathbf{F}$ should be minimized by the PID controller but is not exactly zero, so it still contributes to the total moment.

Validation Procedure. The accuracy of the SpineBot stiffness measurement was quantified by two reference systems. First, we used a surrogate model of the spine based on torsional springs of constant stiffness. Second, we used ovine specimens to characterize the stiffness measurement.

Three different rotational springs were used for the first characterization of SpineBot measurements (Durovis, Perlen, Switzerland). Torsional spring stiffness was 0.23 N·m/deg, 0.32 N·m/deg, and 0.59 N·m/deg—a range similar to human spinal stiffness.

SpineBot measurements were performed on each spring along the lateral bending direction. The stiffer spring was then measured with the SpineBot in different configurations, corresponding to the operation of the robot along each of the anatomical axes, so the SpineBot tested the same spring several times. The relative attachment of the spring to the SpineBot changes so we could test the SpineBot for motions corresponding to the three anatomical axes.

The second validation scenario was based on five functional spine units obtained from four ovine specimens. CT images of the specimens were taken (Somatom Definition AS, Siemens Healthcare GmbH, Erlangen, Germany) at an in-plane resolution of 0.33 mm × 0.33 mm and a slice thickness of 1 mm. CT data was segmented with Amira (Thermo Fisher Scientific, Waltham, MA). Specimens were then dissected to the bone. To minimize changes in lateral stiffness caused by damaged ligaments, we removed the intertransverse ligaments and facet joints. The segments between vertebras T13 and L5 were tested; for each tested segment, the bone and adjacent discs were immobilized with K-wire and embedded into PMAA, leaving only one disc free to move during the measurements. To limit drying of the intervertebral disc, the samples were kept moist with a gauge saturated of saline solution wrapped around the disc during the complete duration of the testing.

The stiffness of the ovine specimens was first evaluated on a SLS. This device is considered the reference standard for measuring spinal stiffness ex vivo [27,28]. The SLS can apply unconstrained pure moments to the spinal segment. Pure bending moments were applied with the SLS in flexion/extension, lateral bending, and axial rotation at a rotation speed of 0.5 deg/s up to angles of ± 5 deg in flexion/extension, ± 7 deg in lateral bending, and ± 2.5 deg in axial rotation. Four load cycles were applied on each motion segment. The testing procedure for the SLS measurements follows the standard protocol for ex vivo spinal testing, where pure moments are applied along the main anatomical axes [28–30]. However, to ensure that the samples were not damaged during SLS testing, we only applied torques in a range below 2 N·m, which is relatively low compared to other studies (± 7.5 N·m [29], 6 N·m [30], or ± 5 N·m [28]). Also, the moment–angle curves produced by the SLS for successive load cycles were checked to identify possible damage of the specimens.

SpineBot stiffness measurements were performed in six steps: (1) the robot was initialized and "homed" to determine its reference position; (2) the robot was attached to the specimen using the haptic mode and air-pressured fixation; (3) the weight of the SpineBot was counterbalanced using the weight canceling platform; (4) the force/torque sensor was zeroed; (5) an optical tracking camera and pointer identified the reference points on the robot to determine the main anatomical axes; and (6) the specimen was loaded along the chosen anatomic axis. We repeated each measurement four times. While the SpineBot had to be repositioned on the spring models to test the different loading orientations, the robot needed only to be fixed once to the ovine specimen to evaluate the three loading directions. For safety reasons, we limited angular velocity to 0.15 deg/s during measurements.

Data Analysis. The data from the load cell were filtered with a sixth-order low-pass Butterworth filter that had a cutoff frequency of 0.1 Hz. The moment at the center of the specimen was then calculated using Eq. (1). Stiffness values obtained with the SpineBot were compared to the reference values obtained with the SLS.

For validation based on the torsion spring, the moment/angle relationship was linear so each measurement returned a single stiffness, which was determined as the slope of the line that best fit the moment/angle relationship.

Since the ovine specimens exhibited nonlinear stiffness and viscoelastic hysteresis, we fitted a cubic function to the average moment/angle relation of both the SpineBot and SLS measurement and determined stiffness as the slope of this cubic function. Spinal stiffness, measured with the SpineBot and SLS, was compared at five angles of rotation equally spaced between the minimal and maximal rotation recorded during the SpineBot measurement. MATLAB R18b (The MathWorks, Inc., Natick, MA) was used for all data analysis.

Results

Each of the six actuators can develop a force up to 150 N. With this configuration, torques up to 10 N·m could be applied along all anatomical axes. The SpineBot's range of motion was different for each anatomical axis. The range of motion was calculated for each load case based on all the SpineBot measurements performed on the ovine specimens. The amount of rotation was the largest in lateral bending (min angle: −5.9 deg ± 0.2 deg, max angle: 5.6 deg ± 0.2 deg), followed by flexion/extension (min angle: −2.2 deg ± 0.5 deg, max angle: 2.4 deg ± 0.2 deg), and the lowest amount of rotation was recorded in axial rotation (min angle: −1.1 deg ± 0.3 deg, max angle: 1.4 deg ± 0.3 deg).

The SpineBot accurately measured the stiffness of the three springs for measurements performed in the lateral bending direction (Fig. 3(*a*)); relative stiffness measurement error was under 5%. Relative error on the average measurement was under 4% for measurements performed in flexion/extension and axial rotation (Fig. 3(*b*)), but standard deviation across consecutive measurements was larger than in lateral bending, especially in the flexion/extension, where standard deviation reaches about 10% of the reference stiffness (Fig. 3(*b*)).

Stiffness of the five ovine specimens was measured with the SpineBot and the SLS (Fig. 4). The SpineBot reproduced the SLS measurement; accuracy was higher in lateral bending and to a lesser extent in axial rotation, where the SpineBot could capture the hysteresis the SLS measured (Fig. 4). But the SpineBot measurements were noisier than the SLS measurements, especially in flexion/extension and axial rotation.

The SpineBot also captured the differing levels of stiffness in the ovine specimens. For all cases, axial stiffness was about five times higher than stiffness in other directions, reaching 1 N·m/deg (Fig. 5). Again, measurement accuracy was higher for lateral bending than for flexion/extension and axial rotation. Correlation between SpineBot and SLS measurements was high ($R^2 > 0.8$), and the slope of the linear regression was close to one for the three anatomical directions (Fig. 5).

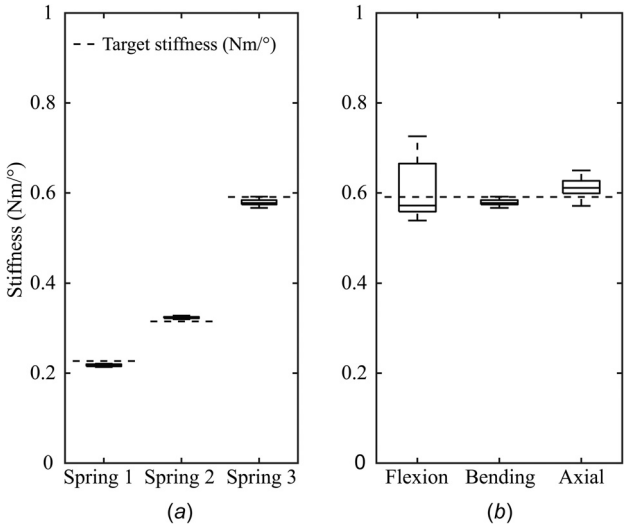

Fig. 3 Stiffness of three torsion springs measured with the SpineBot in a lateral bending configuration and compared to their corresponding reference value (*a*). The SpineBot rotated along all anatomical directions to evaluate the stiffer spring; flexion/extension; lateral bending; and, axial rotation (*b*).

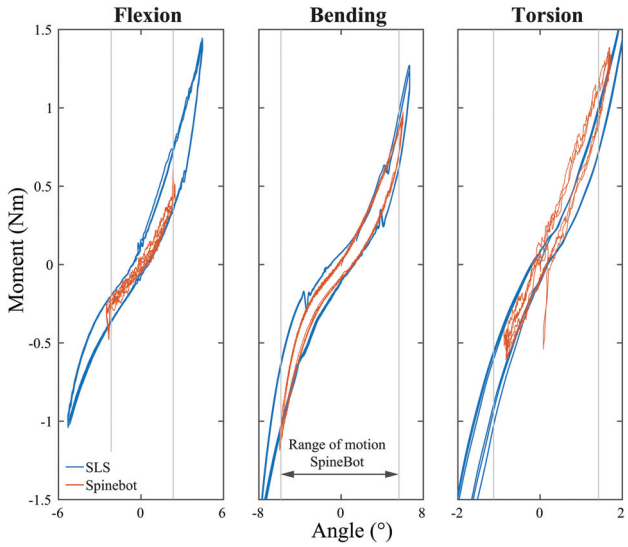

Fig. 4 Raw moment/angle relationship measured during one repetition on one ovine specimen (#149 L4L5) obtained with the SpineBot and the SLS along each anatomical axis. The SLS measurements followed the standard protocol and were limited to moments of ±2 N·m for each anatomical direction. Therefore, the range of motion along each axis is determined by the stiffness of the specimen, while the range of motion of the SpineBot (indicated by two vertical lines on the figure) is controlled by the displacement of its axes. In addition, the range of rotation of the SpineBot is mechanically constrained by the robot design and geometry. This difference explains the larger range of motion recorded for the SLS measurements compared to the SpineBot. In addition, the initial positioning of the SpineBot with respect to the main anatomical direction affects the amount of rotation that it can generate in the positive and negative directions. Consequently, the amount of rotation in the positive direction might differ from the rotation achieved in the negative direction, resulting in the asymmetric loading curve visible on this specimen in the axial direction.

Discussion

We developed a robotic system to quantify spinal stiffness in vivo. Characterizing the system with ex vivo specimens revealed an accuracy comparable to reference measurement systems in current use, but SpineBot's design allows flexible in vivo measurement, a feature not available in other devices.

Since human specimens are difficult to obtain, we used an animal model to evaluate the accuracy of SpineBot measurements. The ovine models we used were less stiff than human spines ex vivo; human spines are about 0.75 N·m/deg when ligaments are removed and about 1.5 N·m/deg when lumbar spines are intact [28,31]. Higher stiffness values were also reported for scoliotic thoracic spines in vivo (about 1.2 N·m/deg at 1 N·m [25]). Despite this difference, the motion characteristics of ovine spines are qualitatively similar to human specimens [32]: axial rotation is small for both species, and flexion and lateral bending range of motion is larger. Although the anatomy of ovine vertebras differs from human vertebras, endplate to disc height is similar [9]. This animal model was already used to validate an intraoperative measurement system [24], thus we consider sheep spines a valid model for this study. The SpineBot was designed to apply torque up to 10 N·m in all directions, so we can quantify stiffer specimens in the future.

Although SpineBot can measure the stiffness with six degree-of-freedom, only the three rotational degrees-of-freedom are relevant for spinal biomechanics. Unlike articular joints, adjacent vertebras are connected to each other by intervertebral discs. These discs constrain the relative vertebral motion, which predominantly occurs in rotation with only a very limited amount of translation. Therefore, the existing biomechanical testing systems designed to quantify spinal stiffness focused on the quantification of its rotational stiffness. We used the same approach for the SpineBot and focused on the characterization of its rotational behavior. In addition, imposing unphysiological motions, such translations between adjacent vertebras, puts the patient at great risks of spinal cord damage.

The mechanical design of the SpineBot limits its range of motion to about 2.5–4.5 deg in flexion and axial rotation. Although this range of motion appears small, another study used a similar range of motion to quantify spinal stiffness in vivo [25]. In addition, the smaller range of motion reported in axial rotation correspond to the stiffest direction tested, which also implies a lower physiological range of motion. This reduced range of motion also represents a safety measure that reduces the risk of damaging tissues, especially the spinal cord, when stiffness is measured in vivo. Nevertheless, a slightly larger amplitude of motion in axial rotation could increase the accuracy of these measurements. Because the SpineBot was positioned above the spine, range of motion in the lateral bending direction was greater than in the other two loading directions. This asymmetry results from the orientation of the axis of rotation, which extends across the center of the robot in lateral bending but is about 15 cm away from the robot for other loading directions (Fig. 1(*b*)); in this case, the axes do not have to extend as much to generate a lateral bending rotation as they do for flexion/extension and axial rotation.

Patient safety was central to SpineBot development. The surgeon controls the operation with a dead-man switch activated at

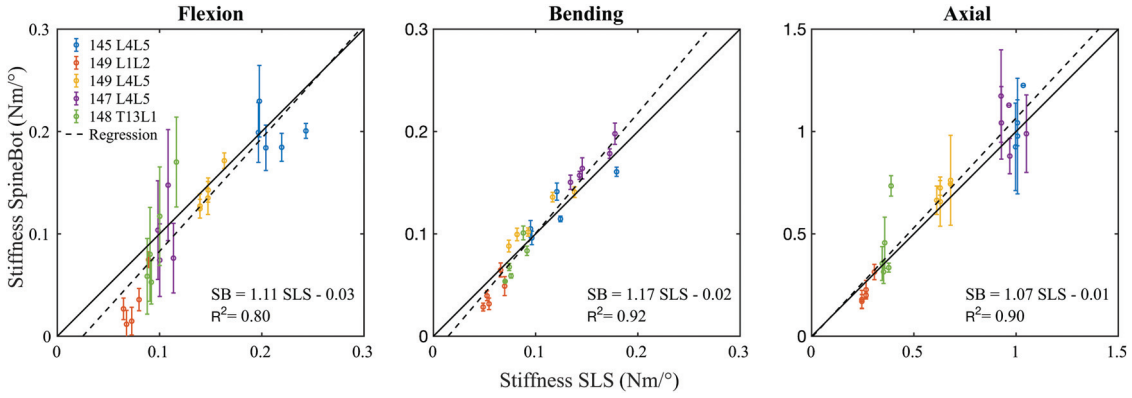

Fig. 5 Comparison of the stiffness measurement between the SpineBot and the SLS on five ovine specimens. Measurements were performed in flexion/extension, lateral bending, and axial rotation. The linear correlation showed a good agreement between both measurement methods with a coefficient of determination higher than 0.8.

different levels: (i) no operation; (ii) operation according to plan; and (iii) emergency stop when the air pressure in the attachment system is interrupted, which immediately detaches the robot from the patient. The surgeon can instantly react to problems. The major risk SpineBot poses is damage to the spinal cord, so the spinal cord will be constantly monitored during surgery to detect potential risk of injury during the measurement process.

The SpineBot preserves a sterile environment. The passive system that attaches the robot to the spine is separate from its active parts, so both parts remain sterile. To keep the active part of the system sterile, a sterile plastic bag is wrapped around the robot. The metal components that attach the system to the patients can be steam sterilized and connected to the robot through the sterile bag.

SpineBot control is critical. Traditional SLS systems aim at applying a pure moment on the tested specimens, but the center of rotation of the spine is unknown and changes during testing. This is why the PID controller is designed to constantly cancel the forces measured by the load cell. If the force is not exactly zero, it contributes to the total moment measured at the center of the motion segment (1). Since the position of the center of rotation is only approximate, the force-induced moment is also an approximation of the contribution of the forces to the total moment. Overall measurement is more accurate if the PID controller cancels the forces; it does so more efficiently for lateral bending moments than for flexion or axial rotation because small elongations of the axes are required to generate spinal rotation in bending. Imperfect cancellation could explain the larger standard deviation we observed for measurements in flexion and axial rotation.

The mechanical response of the spine also poses a challenge for the controller. Because spinal stiffness is nonlinear and unknown before the measurements, it is difficult to determine the optimal set of PID parameters to cancel reaction force, and this also makes stiffness measurements less precise.

But the stiffness we measured with the SpineBot strongly correlated to our reference measurements and could be used to distinguish specimens of varying stiffness. Stiffness measures the local derivative of recorded force/displacement; since it is sensitive to small measurement inaccuracies, it is a demanding metric for evaluating the performance of our system.

Since no system is currently able to measure the spinal stiffness in vivo, it is difficult to comment on the accuracy required for the different clinical applications. Considering the range of stiffness published in the literature, we believe that the level of accuracy reported for the SpineBot is sufficient to enable the stratification of the patients in different treatment groups. This level of accuracy should also enable a suitable description of the stiffness in the population, and could be used to determine the requirements for novel implants and to performed in silico evaluations.

Our vision is that in the future, intra-operative assessment of patient biomechanics will be combined with current standard preoperative imaging techniques to provide the surgeon with a complete picture of the patient's condition. Mechanics is an important part of orthopedic assessment, but no tools are available to quantitatively measure the mechanical state of the tissue for each specific patient. The SpineBot provides capabilities similar to spinal loading simulators, but in vivo, which enable the study of the mechanical properties in a natural physiologic environment, testing of individuals at any age, focus on pathology of choice, and study the impact of surgical action on the stiffness of functional spinal units by pre- and postintervention measurements.

Several clinical applications could directly benefit from a better understanding from these measurements. For example, the treatment of degenerative spine disorders, which represent an increasing health burden for our aging population, could rely on stiffness information. Dynamic transpedicular stabilization could be used to replace the traditional lumbar fusion in the treatment of degenerative instabilities for determined range of segmental stiffness values. Another possible application concerns the planning of deformity correction in pediatric patients with scoliosis. Spinal fusion still represents the treatment of choice in case of progressive curves, independent of the etiology of the deformity. Planning of the surgery requires a good understanding of both patient-specific spinal morphology and stiffness. However, based on routine preoperative clinical and radiographic assessment, the surgeons only have limited information on the mechanical behavior of the patient's spine, since there is no clinical tool able to quantify spinal stiffness in vivo. This mechanical evaluation is expected to enable targeted instrumentation and preserve patient's mobility.

Conclusion

Bone fusion is commonly used to surgically treat spinal disorder, but it can limit a patient's mobility and is frequently associated with degeneration of the adjacent levels [33,34]. To develop nonfusion approaches, we need to better understand the biomechanical characteristics of pathological motion segments. We designed SpineBot to allow clinicians to intraoperatively characterize three-dimensional spinal biomechanics. Validation showed that SpineBot's stiffness measurement is close to the reference standard for ex vivo measurement, and SpineBot can collect this data in the natural physiological environment from patients with the relevant pathology.

Acknowledgment

This work was supported in part by the Swiss National Science Foundation Grant No. 320030_15336 and by the Research Fund of the University of Basel.

Funding Data

- Schweizerischer Nationalfonds zur Förderung der Wissenschaftlichen Forschung (Grant No. 320030_15336; Funder ID: 10.13039/501100001711).
- Universität Basel (Research Fund) (Funder ID: 10.13039/100008375).

References

[1] McCarthy, I., Hostin, R., O'Brien, M., Saigal, R., and Ames, C. P., 2013, "Health Economic Analysis of Adult Deformity Surgery," Neurosurg. Clin. North Am., **24**(2), pp. 293–304.

[2] Wieser, S., Horisberger, B., Schmidhauser, S., Eisenring, C., Brügger, U., Ruckstuhl, A., Dietrich, J., Mannion, A. F., Elfering, A., Tamcan, O., and Müller, U., 2011, "Cost of Low Back Pain in Switzerland in 2005," Eur. J. Health Econ., **12**(5), pp. 455–467.

[3] Dagenais, S., Caro, J., and Haldeman, S., 2008, "A Systematic Review of Low Back Pain Cost of Illness Studies in the United States and Internationally," Spine J., **8**(1), pp. 8–20.

[4] Gédet, P., Thistlethwaite, P. A., and Ferguson, S. J., 2007, "Minimizing Errors During In Vitro Testing of Multisegmental Spine Specimens: Considerations for Component Selection and Kinematic Measurement," J. Biomech., **40**(8), pp. 1881–1885.

[5] Goertzen, D. J., Lane, C., and Oxland, T. R., 2004, "Neutral Zone and Range of Motion in the Spine Are Greater With Stepwise Loading Than With a Continuous Loading Protocol. An In Vitro Porcine Investigation," J. Biomech., **37**(2), pp. 257–261.

[6] Lysack, J. T., Dickey, J. P., Dumas, G. A., and Yen, D., 2000, "A Continuous Pure Moment Loading Apparatus for Biomechanical Testing of Multi-Segment Spine Specimens," J. Biomech., **33**(6), pp. 765–770.

[7] Patwardhan, A. G., Havey, R. M., Meade, K. P., Lee, B., and Dunlap, B., 1999, "A Follower Load Increases the Load-Carrying Capacity of the Lumbar Spine in Compression," Spine, **24**(10), pp. 1003–1009.

[8] Wilke, H. J., Claes, L., Schmitt, H., and Wolf, S., 1994, "A Universal Spine Tester for In Vitro Experiments With Muscle Force Simulation," Eur. Spine J., **3**(2), pp. 91–97.

[9] Thompson, R. E., Barker, T. M., and Pearcy, M. J., 2003, "Defining the Neutral Zone of Sheep Intervertebral Joints During Dynamic Motions: An In Vitro Study," Clin. Biomech., **18**(2), pp. 89–98.

[10] Stokes, I. A., Gardner-Morse, M., Churchill, D., and Laible, J. P., 2002, "Measurement of a Spinal Motion Segment Stiffness Matrix," J. Biomech., **35**(4), pp. 517–521.

[11] Panjabi, M. M., 1988, "Biomechanical Evaluation of Spinal Fixation Devices—I: A Conceptual Framework," Spine, **13**(10), pp. 1129–1134.

[12] Brown, M. D., Wehman, K. F., and Heiner, A. D., 2002, "The Clinical Usefulness of Intraoperative Spinal Stiffness Measurements," Spine, **27**(9), pp. 959–961.

[13] Krenn, M. H., Ambrosetti-Giudici, S., Pfenniger, A., Burger, J., and Piotrowski, W. P., 2008, "Minimally Invasive Intraoperative Stiffness Measurement of Lumbar Spinal Motion Segments," Neurosurgery, **63**(4), pp. 309–313.
[14] Kanayama, M., Hashimoto, T., Shigenobu, K., Oha, F., Ishida, T., and Yamane, S., 2003, "Intraoperative Biomechanical Assessment of Lumbar Spinal Instability: Validation of Radiographic Parameters Indicating Anterior Column Support in Lumbar Spinal Fusion," Spine, **28**(20), pp. 2368–2372.
[15] Ebara, S., Harada, T., Hosono, N., Inoue, M., Tanaka, M., Morimoto, Y., and Ono, K., 1992, "Intraoperative Measurement of Lumbar Spinal Instability," Spine, **17**(Suppl. 3), pp. S44–S50.
[16] Hasegewa, K., Kitahara, K., Hara, T., Takano, K., and Shimoda, H., 2009, "Biomechanical Evaluation of Segmental Instability in Degenerative Lumbar Spondylolisthesis," Eur. Spine J., **18**(4), pp. 465–470.
[17] Brown, M. D., Holmes, D. C., and Heiner, A. D., 2002, "Measurement of Cadaver Lumbar Spine Motion Segment Stiffness," Spine, **27**(9), pp. 918–922.
[18] Brown, M. D., Holmes, D. C., Heiner, A. D., and Wehman, K. F., 2002, "Intraoperative Measurement of Lumbar Spine Motion Segment Stiffness," Spine, **27**(9), pp. 954–958.
[19] Kanayama, M., Abumi, K., Kaneda, K., Tadano, S., and Ukai, T., 1996, "Phase Lag of the Intersegmental Motion in Flexion-Extension of the Lumbar and Lumbosacral Spine. An In Vivo Study," Spine, **21**(12), pp. 1416–1422.
[20] Rohlmann, A., Gabel, U., Graichen, F., Bender, A., and Bergmann, G., 2007, "An Instrumented Implant for Vertebral Body Replacement That Measures Loads in the Anterior Spinal Column," Med. Eng. Phys., **29**(5), pp. 580–585.
[21] Rohlmann, A., Graichen, F., Bender, A., Kayser, R., and Bergmann, G., 2008, "Loads on a Telemeterized Vertebral Body Replacement Measured in Three Patients Within the First Postoperative Month," Clin. Biomech., **23**(2), pp. 147–158.
[22] Rohlmann, A., Graichen, F., Kayser, R., Bender, A., and Bergmann, G., 2008, "Loads on a Telemeterized Vertebral Body Replacement Measured in Two Patients," Spine, **33**(11), pp. 1170–1179.
[23] Rohlmann, A., Zander, T., Graichen, F., Dreischarf, M., and Bergmann, G., 2011, "Measured Loads on a Vertebral Body Replacement During Sitting," Spine J., **11**(9), pp. 870–875.
[24] Reutlinger, C., Gédet, P., Büchler, P., Kowal, J., Rudolph, T., Burger, J., Scheffler, K., and Hasler, C., 2011, "Combining 3D Tracking and Surgical Instrumentation to Determine the Stiffness of Spinal Motion Segments: A Validation Study," Med. Eng. Phys., **33**(3), pp. 340–346.
[25] Reutlinger, C., Hasler, C., Scheffler, K., and Büchler, P., 2012, "Intraoperative Determination of the Load-Displacement Behavior of Scoliotic Spinal Motion Segments: Preliminary Clinical Results," Eur. Spine J., **21**(Suppl 6), pp. 860–867.
[26] Harib, K., and Srinivasan, K., 2003, "Kinematic and Dynamic Analysis of Stewart Platform-Based Machine Tool Structures," Robotica, **21**(5), pp. 541–554.
[27] Hermann, A., Voumard, B., Waschk, M. A., Hettlich, B. F., and Forterre, F., 2018, "In Vitro Biomechanical Comparison of Four Different Ventral Surgical Procedures on the Canine Fourth-Fifth Cervical Vertebral Motion Unit," Vet. Comp. Orthop. Traumatol., **31**(6), pp. 413–421.
[28] Stadelmann, M. A., Maquer, G., Voumard, B., Grant, A., Hackney, D. B., Vermathen, P., Alkalay, R. N., and Zysset, P. K., 2018, "Integrating MRI-Based Geometry, Composition and Fiber Architecture in a Finite Element Model of the Human Intervertebral Disc," J. Mech. Behav. Biomed. Mater., **85**, pp. 37–42.
[29] Wilson, D. C., Niosi, C. A., Zhu, Q. A., Oxland, T. R., and Wilson, D. R., 2006, "Accuracy and Repeatability of a New Method for Measuring Facet Loads in the Lumbar Spine," J. Biomech., **39**(2), pp. 348–353.
[30] Stadelmann, M. A., Stocker, R., Maquer, G., Hoppe, S., Vermathen, P., Alkalay, R. N., and Zysset, P. K., 2020, "Finite Element Models Can Reproduce the Effect of Nucleotomy on the Multi-Axial Compliance of Human Intervertebral Discs," Comput. Methods Biomech. Biomed. Eng., **23**(13), pp. 934–944.
[31] Heuer, F., Schmidt, H., Klezl, Z., Claes, L., and Wilke, H.-J., 2007, "Stepwise Reduction of Functional Spinal Structures Increase Range of Motion and Change Lordosis Angle," J. Biomech., **40**(2), pp. 271–280.
[32] Wilke, H. J., Kettler, A., and Claes, L. E., 1997, "Are Sheep Spines a Valid Biomechanical Model for Human Spines?," Spine, **22**(20), pp. 2365–2374.
[33] Goffin, J., Geusens, E., Vantomme, N., Quintens, E., Waerzeggers, Y., Depreitere, B., Van Calenbergh, F., and van Loon, J., 2004, "Long-Term Follow-Up After Interbody Fusion of the Cervical Spine," J. Spinal Disord. Tech., **17**(2), pp. 79–85.
[34] Ghiselli, G., Wang, J. C., Bhatia, N. N., Hsu, W. K., and Dawson, E. G., 2004, "Adjacent Segment Degeneration in the Lumbar Spine," J. Bone Jt. Surg. Am., **86**(7), pp. 1497–1503.